Evaluation of Blue and Green Absorbing Proteorhodopsins as Holographic Materials

Bangwei Xi,[†] William C. Tetley,[‡] Duane L. Marcy,[‡] Cheng Zhong,[§] Gregg Whited,[⊥] Robert R. Birge,[#] and Jeffrey A. Stuart*[,†,§,#]

W.M. Keck Center for Molecular Electronics and Department of Chemistry, Syracuse University, Syracuse, New York 13244; Department of Electrical & Computer Engineering, Syracuse University, Syracuse, New York 13244; Institute of Materials Science, University of Connecticut, Storrs, Connecticut 06269; Genencor International, Inc., Palo Alto, California 94304; and Department of Chemistry, University of Connecticut, Storrs, Connecticut 06269

Received: May 25, 2007; In Final Form: October 26, 2007

Transient holographic diffraction is observed for the green (GPR) and blue (BPR) absorbing proteorhodopsins (BAC31A8 and HOT75M1, respectively), as well as the GPR E108Q and BPR E110Q variants. In contrast to bacteriorhodopsin, where the metastable bR−M pair is responsible for generating diffraction, the pR and red-shifted N-like states fulfill that role in both the green and blue wild-type proteorhodopsins. The GPR E108Q and BPR E110Q variants, however, behave more similarly to their bacteriorhodopsin analogue, D96N, with diffraction arising from the PR M-state (strongly enhanced in both GPR E108Q and BPR E110Q). Of the four proteins evaluated, wild type (WT) GPR and GPR E108Q produce the highest diffraction efficiencies, η_{max}, at ∼1% for a 1.7 OD sample. GPR E108Q, however, requires 1−2 orders of magnitude less laser intensity to generate η equivalent to WT GPR and BR D96N under similar conditions (as compared to literature values). WT BPR requires lower actinic powers than GPR but diffracts only about 30% as well. BPR E110Q performs the most poorly of the four, with $\eta_{max} < 0.05\%$ for a 1.4 OD film. The Kramers−Kronig transformation and Koglenik's coupled wave theory were used to predict the dispersion spectra and diffraction efficiency for the long M-state variants. To a first approximation, the gratings formed by all samples decay upon discontinuing the 520 nm actinic beams with a time constant characteristic of the appropriate intermediate: the N-like state for WT GPR and BPR and the M-state for GPR 108Q and BPR E110Q.

Introduction

Proteorhodopsin (PR), an archaeal rhodopsin and marine analogue of bacteriorhodopsin (BR), was first discovered in the genome of an uncultivated member of the marine γ-proteobacterial SAR86 group collected from Monterey Bay.[1] Soon thereafter, new PR variants were identified at various marine locations and depths,[2−4] including the cultivated marine bacteria SAR11,[5] which is possibly the most abundant bacteria on the planet. And recently, shotgun sequencing techniques applied to marine samples from a variety of ocean locations have revealed that this protein family has an abundance far greater than previously thought, with PR-gene sequences numbering in the thousands.[6,7] Proteorhodopsin is composed of a single 249-amino acid polypeptide chain with a native molecular weight of 27 kDa, as determined by DNA sequence.[1] On the basis of the absorption maximum at alkaline pH, proteorhodopsin can be divided into two subgroups: green (GPR) and blue (BPR). GPR can generally be found at the ocean surface and has an absorption maximum of 520 nm, while BPR is present at greater depths and absorbs maximally at 490 nm.

Holography has many promising applications, including data storage, real-time microscopic imaging, and optical processing. Transition-metal or rare-earth ion doped photorefractive crystal-based holographic three-dimensional data storage has been studied extensively—examples of such materials include iron-doped lithium niobate, strontium barium niobate, and barium titanate, doped with iron, cesium, or manganese.[8] The estimated information density is far more than traditional platter architectures,[9] but cost, processing, and reusability issues have precluded commercialization. Bacteriorhodopsin has long been considered a good candidate material for device applications due to its unique photochemical properties, including high sensitivity, high cyclicity, and good thermal stability.[10−17] BR-based holography has been a subject of active interest for well over a decade,[18−25] with the promises of ultrahigh storage density (5000 lines/mm), full write−read−erase capabilities, and excellent potential for fine-tuning performance through genetic modification.[15,18−22,25−33] The earliest attempts utilized the wild-type protein to generate real-time holographic gratings between the bR resting state and the M-state, with the lifetime of the latter often enhanced by the addition of various amines.[29,34,35] The genetically engineered BR variant D96N has attracted special attention due to its prolonged M-state and has even been utilized in a commercial holographic interferometer designed for nondestructive testing.[10] The prolonged M-state lifetime (up to several minutes) gives the resulting holographic material high sensitivity and acceptable diffraction efficiency (as high as 7% in a 5 OD film[19]). For the sake of comparison, the diffraction efficiency observed in the wild type protein is approximately half of that generated by D96N (given equivalent optical densities).[18] Permanent holography based on BR has been a

* Corresponding author. E-mail: jeffrey.stuart@uconn.edu.
[†] W.M. Keck Center for Molecular Electronics and Department of Chemistry, Syracuse University.
[‡] Department of Electrical & Computer Engineering, Syracuse University.
[§] Institute of Materials Science, University of Connecticut.
[⊥] Genencor International, Inc.
[#] Department of Chemistry, University of Connecticut.

10.1021/jp0740752 CCC: $40.75 © 2008 American Chemical Society
Published on Web 02/01/2008

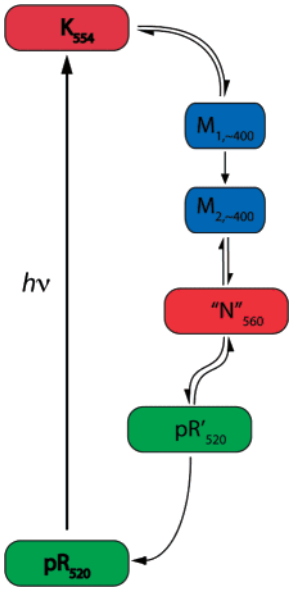

Figure 1. Approximate green proteorhodopsin (BAC31A8) photocycle and retinal λ_{max} in nm, based upon Váró et al.[40] There is a minimum of four intermediates, but as many as seven have been reported.[41] Unlike the bacteriorhodopsin photocycle, there is no L state that can be observed either kinetically[40] or at low temperatures (in-house observations). The pR′ intermediate was identified kinetically and is analogous at least in part to the BR O state (based on FTIR studies[40,41]). However, unlike the BR O state, pR′ is spectrally indistinguishable from the pR resting state. Similarly, only one M state is observed spectroscopically, although kinetic data are better explained by including two M states.[40]

more elusive goal, although approaches have included utilization of the branched photocycle[36,37] or irreversible photoconversion into a permanent red-shifted state (F620).[31] However, high light intensities and/or prolonged exposures are required for sufficient photoconversion into a permanent state,[37] which mandates the use of large lasers in the optical layout. This requirement alone precludes BR for commercial device applications, in the absence of a suitably optimized variant. Although progress along these lines is good,[32,38,39] exploration of other systems is warranted.

Proteorhodopsin has been shown to have photochemical properties similar to bacteriorhodopsin,[4,40−43] including a common chromophore and structural motif, proton-pump activity (across the cell membrane from the cytoplasmic side to the extracellular side upon light absorption), and a photocycle composed of several spectroscopically distinct intermediates (pR, K, M, and a red-shifted intermediate analogous to the BR N and/or O states, Figure 1). The Schiff base proton acceptor and donor in green proteorhodopsin are Asp-97 and Glu-108, respectively (Asp-99 and Glu-110 in blue proteorhodopsin), analogous to Asp-85 and Asp-96 in BR,[44,45] indicating that these proteins operate with similar mechanisms. Unlike bacteriorhodopsin, however, the primary photoproduct accumulated during the photocycle at alkaline pH in both the wild type GPR and BPR proteins is a red-shifted intermediate (similar to the BR N-state), while the M-state does not accumulate due to fast thermal decay.[40,41,45] If the proton donor to the Schiff base is mutated to glutamine in either protein (GPR E108Q or BPR E110Q, both analogous to BR D96N), the yield and lifetime of M-state is significantly improved. In these variants, nearly all the resting state can be photoconverted to M upon illumination.

On the basis of the remarkable similarity of these proteins, it follows that the proteorhodopsins may have similar potential to bacteriorhodopin in device architectures, including holographic memory storage. Proteorhodopsin may have more potential than bacteriorhodopsin based on several key observations concerning ease of production, diversity, and relative stability. Because all PR to date has been expressed heterologously in *E. coli*, larger quantities of the protein can be produced more quickly and efficiently than currently possible for BR, which is of obvious importance for applications with commercial potential. In addition, PR has proven to be a member of an extremely diverse family of proteins, with nearly 3000 naturally occurring variants already identified,[3,6,45−51] and promises to be just as flexible as BR from the standpoint of genetic modification. Last, detergent-solubilized proteorhodopsin appears to be as stable as BR in the purple membrane. In contrast, BR's stability is considerably reduced once removed from the purple membrane;[52] use of the solubilized protein could be important in volumetric holographic and other optical applications where purple membrane patches will potentially introduce light scattering, thereby degrading efficiency. PR-containing films prepared in-house consistently scatter less light than otherwise identical films prepared with BR (data not shown). Liang and co-workers have recently presented evidence that solubilized PR exists as a trimer,[53] which may account for the observed difference in stability as compared to detergent-solubilized, monomeric[53,54] BR; consistent with their observations, detergent-solubilized PR samples in our laboratory have remained viable for at least a year, demonstrating no significant changes in spectral profile or photokinetics (with the exception of BPR E108Q, as discussed below). At present, a formal comparison of the relative stabilities of the membrane-bound proteins is not possible because none of the proteorhodopsins has been characterized in its native organism.

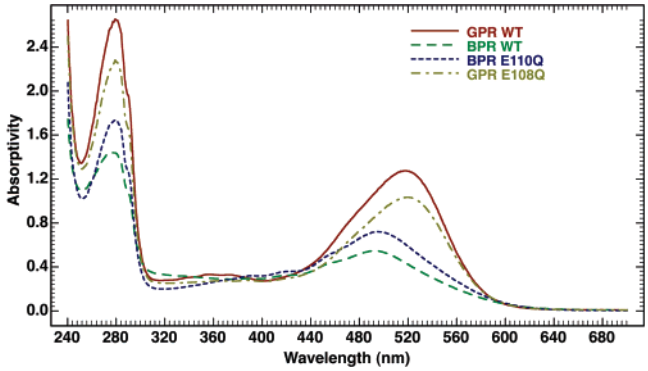

Figure 2. Representative aqueous absorbance spectra of the proteins used in this study (CAPS buffer, pH 10). The optical densities have been adjusted as needed for clarity. Suspending the proteins in poly(acrylamide) gels (spectra not shown) for the experiments resulted in no modification of the absorption profile.

In this paper, we present the experimental demonstration of transient volume diffractive holography in thin proteorhodopsin-polymer gels. Four types of PR were evaluated for these studies, including the wild-type green and blue proteins (BAC31A8, accession no. Q9F7P4, and HOT75M1, accession no. AF349979), and their long M-state variants, GPR E108Q and BPR E110Q.

Materials and Methods

Purified proteorhodopsin was produced and purified as reported previously.[47,51] Representative spectra of the four proteins are shown in Figure 2. A Millipore Centriplus centrifugal filter tube (10 000 MW cutoff) was used to concentrate the protein at 3043 g for 6−8 h, to a final volume of about 200 μL. The concentrated protein was resuspended in 2.5 mL of 100 mM 3-(cyclohexylamino)-1-propanesulfonic acid

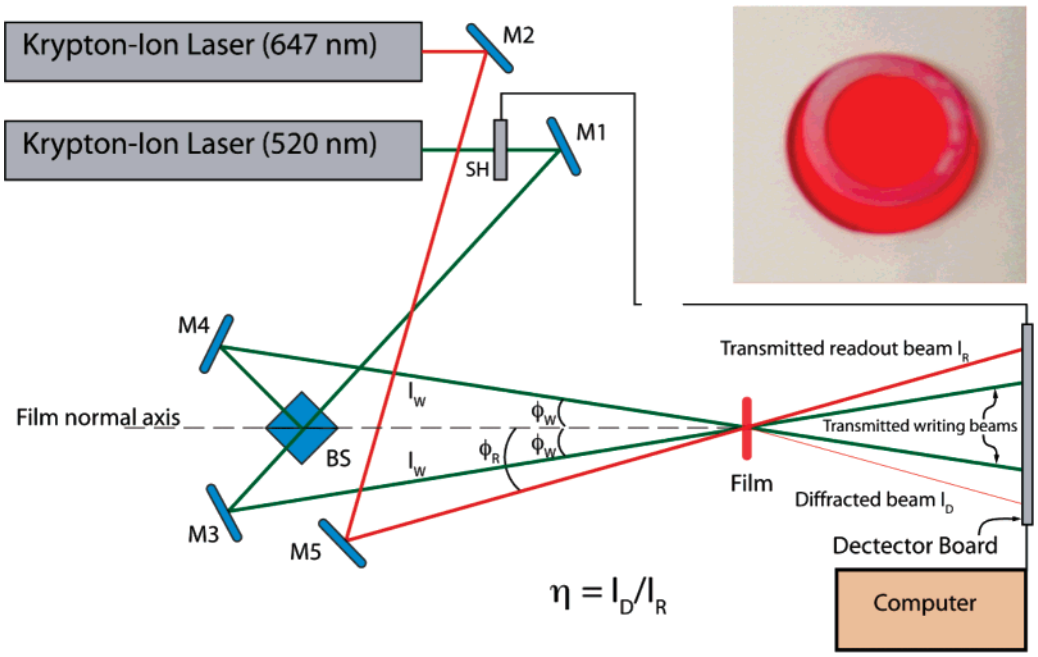

Figure 3. Optical layout for the holographic interferometer. The green 520 nm shutter-controlled (SH) writing beam is split by the beam splitter (BS) into two coherent beams of equal path length, which intersect at the sample film. The beams initiate photochemistry and interfere constructively and destructively within the film—the resulting bright and dark fringes are recorded temporarily as a diffraction pattern. The 647 nm reading beam intersects the film at the Bragg angle (ϕ_R). The intensities of the transmitted writing, reading, and diffracted beams are detected and registered by a detector board made in-house. Diffraction efficiency is defined as the ratio of the diffracted beam intensity, I_D, to that of the transmitted read beam, I_R. The sample (inset) consists of the protein suspended in a poly(acrylamide) film, sandwiched between two BK7 glass discs with a 200 μm path length donut-shaped Teflon spacer.

TABLE 1: Compiled Diffraction Efficiency Data for GPR, BPR, and PR E108Q Variants

proteorhodopsin	OD at λ_{max}[a]	C (mg/mL)[b]	τ_f (ms)[c]	I_W (mW/cm^2)[d]	τ_d (ms)[e]	η_{max}[f] (%)
GPR (BAC31A8)	1.2	0.74	30	30	45	0.6
	1.7	1.1	33	40	47	1.0
BPR (HOT75M1)	1.1	0.68	76	10	255	0.23
	1.7	1.1	78	15	223	0.27
GPR E108Q	1.3	0.81	450	0.3	660	0.5
	2.0	1.2	700	0.4	688	0.7
BPR E110Q	1.4	0.87	<100	1.5	1818	0.04

[a] Retinal chromophore λ_{max}, 520 nm for GPR/GPR E108Q and 490 nm for BPR/BPR E110Q. [b] Based on $\epsilon = 43\,500$ cm^{-1} M^{-1} at λ_{max}, MW = 27 000 g/mol. [c] Formation time at I_W. [d] Combined writing laser intensity at 520 nm necessary to achieve η_{max}. [e] Diffraction decay time upon removal of 520 nm writing beams. [f] Maximum diffraction efficiency achievable prior to grating saturation.

(CAPS) buffer, 1 mL of 40% acrylamide solution containing acrylamide and *N*,*N*′-methylenebis(acrylamide) in a ratio of 29:1 (w/w), and 0.05 mL of tetramethylethylenediamine (TEMED) at a final pH at 10.0. The mixture was concentrated again as described above. The pH was measured after centrifugation to ensure that it had remained constant. The solution was concentrated further using a Millipore MicroCon centrifugal filter device (10 000 MW cutoff) in a Microfuge 18 centrifuge for an additional 30 min (13 000 g). The final volume was ~120 μL. After degassing the solution, 4 μL of 1% (w/w) ammonium persulfate were added to initiate polymerization, followed by rapid agitation. Before polymerization was complete, the solution was carefully transferred into a 200 μm path length donut-shaped Teflon spacer (International Crystal Laboratories) resting on a 1 in. diameter BK-7 glass disk substrate (Esco). The resulting film was quickly covered with another BK-7 glass disk (Figure 3, inset); polymerization was typically completed in several hours. The resulting assembly was placed into an airtight, anodized aluminum retainer, designed and fabricated in-house. The final optical densities (OD) of the films were typically between 1.5 and 2.0, as measured for the retinal chromophore peaks (520 nm for GPR, 490 nm for BPR); optical densities and protein concentrations for each film examined are listed in Table 1).

The optical layout for volume holography is shown in Figure 3. A krypton-ion CW laser (Coherent, Innova 90 series, 520 nm) with an electronically controlled optical shutter (SH) was used to initiate writing. Shutter operation was facilitated by computer control. Following the shutter, the green laser beam was divided into two equal coherent beams (50/50 beam splitter (BS)), which were redirected through mirrors M3 and M4 to an intersection plane at the sample, thereby producing an interference pattern. The incident angle of the writing beam, ϕ_W, was 9.02°. A second krypton-ion laser (Coherent, Innova 300 series, 647 nm) provided the reading beam: the intensity of the reading beam was set to be less than 0.1 mW/cm^2 to avoid detector saturation. The incident angle of the reading beam ϕ_R satisfied the Bragg condition at 11.25°:

$$\lambda_W \sin(\phi_R) = \lambda_R \sin(\phi_W) \quad (1)$$

λ_R and λ_W are defined as the reading (647 nm) and writing (520 nm) wavelengths, respectively, and angles (ϕ_R and ϕ_W) are defined as in Figure 3, the incident angles of the reading and writing beams, respectively. The experimental diffraction ef-

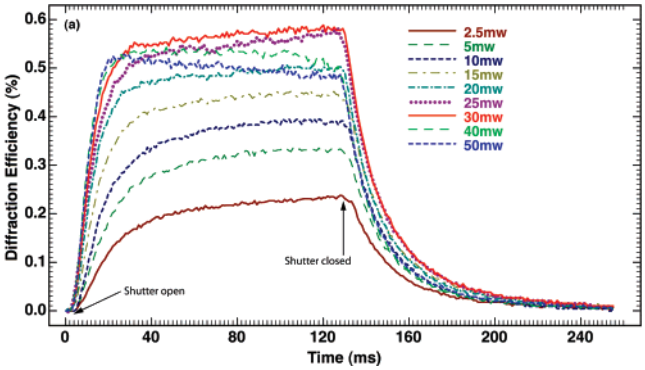

Figure 4. GPR diffraction data for 1.2 OD film at various writing intensities. Saturation starts to occur at writing intensities greater than 30 mW.

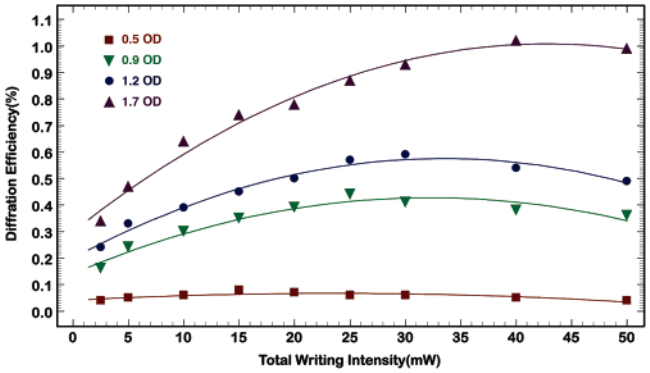

Figure 5. Dependence of diffraction efficiency upon total combined writing intensity (of the two 520 nm actinic beams) for green proteorhodopsin (GPR, BAC31A8).

ficiency (η) is defined as the ratio of the intensity of diffracted beam to that of transmitted reading beam.

$$\eta = I_D/I_R \tag{2}$$

Automated system control and data collection was facilitated by a QBasic program generated in-house. Shutter timing varied as a function of the protein being evaluated. All the measurements were performed in dark and at room temperature without further temperature control.

The Kramers−Kronig transformation was used to predict the change in refractive index associated with phototransformation, and Kogelnik's coupled wave theory was then used to predict the resulting holographic diffraction efficiency (both as described previously[21,27]). Unfortunately, these techniques could only be applied to the long M-state variant proteins because a pure spectrum of the intermediate responsible for generating diffraction in the wild-type proteorhodopsins (the N-like state) could not be obtained without contributions from other states. Supporting Information on the background associated with these calculations is provided.

Results and Discussion

Real-time, transient, diffraction was demonstrated for each of the four proteins evaluated. Transmitted and diffracted beam intensities were detected by photodiodes, which recorded the full time-course of grating formation and decay. The diffraction efficiency (η) for each protein was calculated according to eq 2 and is used herein as an indicator of holographic quality of the various PR films.

Green-Absorbing Proteorhodopsin (GPR, BAC31A8). Typical real-time diffraction data for a wild-type GPR sample with an optical density (OD) at 520 nm of 1.2 are shown in Figure 4 for a variety of actinic laser powers (i.e., writing beam intensities). Upon exposure of the PR film to the 520 nm actinic beams (shutter open), the diffraction efficiency rises exponentially on a millisecond time scale, until it reaches a plateau characteristic of the writing power. Rise time is a function of total laser intensity and sample optical density—higher intensities result in faster formation of diffraction patterns (i.e., more protein can be photoconverted simultaneously), while higher optical densities show the opposite trend (a larger amount of photoconversion is necessary to establish the grating). Cessation of the writing beams (shutter closed) results in an exponential decay of the diffraction pattern as a function of the lifetime of the diffracting state. The diffraction efficiency, η, increases with both total writing intensity (the sum of two writing beam intensities) and protein optical density—this is a simple reflection of the amount of the protein available for photoexcitation. As expected, saturation effects are observed at the higher laser powers, at which point the grating becomes nonsinusoidal as the intensity of the actinic light is too bright for the resulting photochemistry to be confined to the diffraction pattern interference fringes (see the traces at 40 and 50 mW/cm^2 in Figure 4).[19] All the proteins examined showed similar behavior (below), with differences primarily in saturation level and rise and decay times (see Table 1). The dependence of maximum diffraction efficiency (η_{max}) as a function of proteorhodopsin optical density and total (combined) writing intensity is shown in Figure 5. Consistent with the observations described above, the maximum diffraction efficiency is limited by sample optical density (protein concentration), a photostationary state results at each combination of optical density and writing intensity, and the higher the writing intensity, the faster this state is achieved. In all trials, WT GPR shows the highest diffraction efficiency of ~1% at 40 mW/cm^2 from the 647 nm kryton ion line.

Unlike bacteriorhodopsin, the proteorhodopsin photocycle accumulates very little M state, even at alkaline pH.[40,41] However, a red-shifted intermediate comparable to the BR N and O states is produced in relative abundance late in the PR photocycle, absorbing maximally around 590 nm. Given the small amount of M produced in the native photocycle, this late red-shifted intermediate is likely to be responsible for the majority of the observed diffraction in the GPR films. In order to determine the nature of the active state, the thermal decay of the observed diffraction efficiency was examined upon discontinuing the writing/actinic beams. In volume diffraction, when $\eta \ll 1$, the diffracted beam intensity is proportional to the square of the population of the intermediate.[18,55] If there is only one active state contributing to diffraction pattern formation, the thermal decay of the intermediates can be expressed as a first-order reaction with the lifetime τ.

$$\eta(t) \propto \exp^2(-t/\tau) \tag{3}$$

Equation 3 relates the observed signal ($\eta(t)$, the diffraction efficiency at time t) to the lifetime of the photoactive state. Given a single photodiffractive state, a single-exponential fit function should be able to describe the observed decay. A double-exponential fit would support the possibility of two states contributing to the diffraction pattern (i.e., the red-shifted intermediate with a contribution from the M state). Application of eq 3 to both the green and blue proteorhodopins investigated resulted in first-order decays, indicating that either the red-shifted state is the only intermediate involved in the holographic recording process or the contribution of M state is too small to

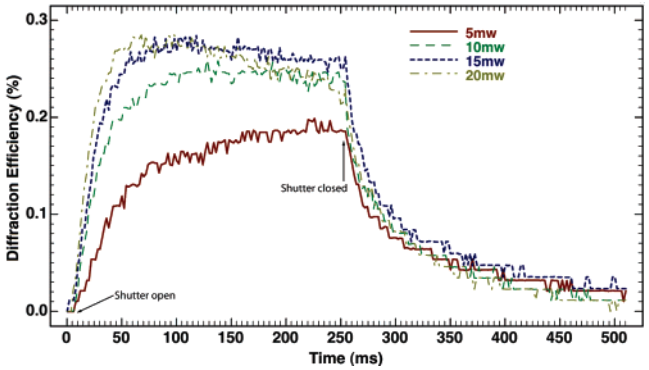

Figure 6. BPR Diffraction data for a 1.7 OD film at various total writing intensities. Saturation is seen at writing intensities greater than 15 mW.

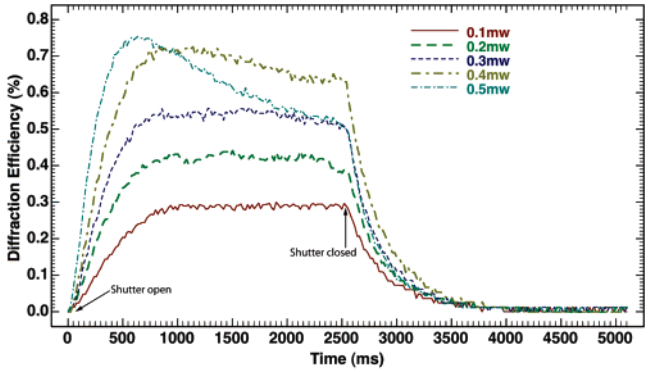

Figure 7. GPR E108Q diffraction data for a 2.0 OD film at various total writing intensities. Although the diffraction efficiency is comparable to that produced by the wild-type protein, the maximum is achieved at intensities 2 orders of magnitude lower.

observe a multiexponential thermal decay. The lifetime shows no dependence on either the total writing intensity or the concentration of the protein (Table 1), averaging 46 ms for GPR. Interpretation of this lifetime is somewhat difficult on the basis of literature values. It is comparable to the decays of the red-shifted intermediates as reported by Friedrich et al.[42] and Dioumaev et al.[41] (ranging from ~40 to 45 ms in both studies, presented here as the sum of the individual lifetimes reported for the primary late-photocycle red-shifted kinetic components) but considerably different than that reported by Váró (~19 ms).[40] Both Dioumaev and Váró identified long-lived time contants of 153 and 230 ms, respectively, for re-formation of the PR resting state (pH 9.5). Váró attributed this state to a spectrally silent PR′ state (520 nm, Figure 1) similar to the BR O state. Váró also identified a 43 ms lifetime for the red-shifted PR K state, which conceivably could contribute to the diffraction in Figure 4, although one would then expect a multiexponential diffraction decay with components from all the red-shifted intermediates (i.e., K and N/O), resulting in a longer lifetime than observed here. The K state was determined to be on a microsecond time scale by both Friedrich and Dioumaev.[41,42] These discrepancies might be attributed to sample preparation, while the first two studies used solubilized protein (as done here), the Váró study employed PR in *E. coli* membranes.

The observation that in proteorhodopsin diffraction likely originates from the N/O state is in contrast to bacteriorhodopsin, where diffraction under identical conditions results from the M-state. As mentioned above, pure spectra of the red-shifted N-like state could not be obtained for either of the wild-type proteins without a contribution from the M state. Therefore, theoretical prediction of diffraction efficiencies through the Kramers−Kronig and Kogelnik equations was not possible. However, such treatments are provided for the GPR E108Q and BPR E110Q variants below.

Blue Absorbing Proteorhodopsin (BPR, HOT75M1). Blue proteorhodopsin has a longer photocycle than GPR or BR, and there is evidence to suggest that it may act in a photosensory capacity.[45,51] Figure 6 shows the diffraction that resulted from a wild-type BPR film with an optical density of 1.7 (490 nm). The traces typically exhibit similar behavior to GPR, although saturation is reached at much lower laser powers. Compared to WT-GPR, WT-BPR needs only 20−30% of the laser intensity to achieve maximum diffraction efficiency at a similar optical density. However, the resulting η_{max} is reduced to ~0.23%, roughly one-quarter of that observed for WT-GPR (Figure 4). A possible explanation for this difference is use of identical writing and reading wavelengths for both proteins—the Krypton ion 520 and 647 nm lines may not be suitable for the blue protein, the green 520 nm line will photoexcite GPR better than BPR (λ_{max} of 520 nm vs 490 nm, respectively), and the 647 nm line might not be a good match for the wavelength-dependent profile of BPR diffraction efficiency. Just as observed for GPR, very little M state accumulates in the BPR photocycle, indicating that the later and more abundant red-shifted intermediate (N/O-like state) is most likely responsible for generating diffraction. In fact, given that diffraction in both wild-type proteins originates from a red-shifted state, the 520 nm write beam might partially be absorbed or initiate unwanted photochemistry, thereby degrading the grating. As for GPR, analysis of BPR using the Kramers−Kronig and Kogelnik equations was not possible because no spectrum of the N-like photoproduct could be generated; all attempts resulted in spectra that had contributions from the M and perhaps even the K states (low-temperature studies, data not shown). Applying eq 3 yields a single-exponential decay with the lifetime of the red-shifted diffracting state calculated to be 255 ms, roughly 6 times slower than observed for GPR but faster than has been previously reported. (Wang et al. reported recovery of the BPR resting state as a function of decay of the O-like intermediate to be a full order of magnitude slower than GPR.[45]) Sample preparation may account for the discrepancy, as the solubilized protein is used herein, and the aforementioned study used BPR in *E. coli* membranes.

GPR E108Q and BPR E110Q. The GPR E108Q and the BPR E110Q variants are equivalent to bacteriorhodopsin D96N and similarly exhibit strongly prolonged M-state lifetimes. Like BR Asp-96, these residues operate as the primary proton donors to the Schiff base in their respective proteins. Mutation of this residue to asparagine (N) in BR greatly reduces the rate of proton transfer, thereby prolonging the lifetime of the blue-shifted M state. BR D96N has been evaluated extensively for transient holographic applications,[10,18−20,22,56,57] and as such, the equivalent mutations in blue and green proteorhodopsin bear investigation.

Figure 7 shows the rise and decay of the diffraction efficiency η for a 1.3 OD_{520} film of GPR E108Q. As compared to wild type GPR, both formation and decay of the diffraction grating occur about 10 times slower (see Table 1). Furthermore, the protein is much more sensitive to light (~50×), requiring dramatically reduced writing intensities—only 0.5 mW/cm^2 or 1% of the intensity to generate the η_{max} in GPR. Whereas the wild-type protein required 20 mW/cm^2 to achieve an efficiency of 0.5% (1.2 OD sample), only 0.4 mW/cm^2 was required for E108Q (at 1.3 OD). The M-state lifetime of GPR E108Q is better than 20 times longer than WT-GPR (Table 1, fit data not

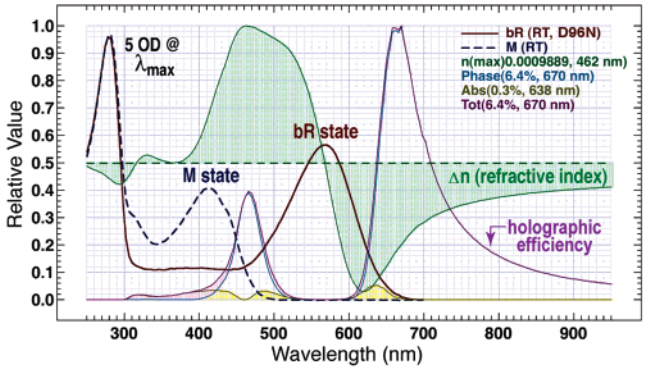

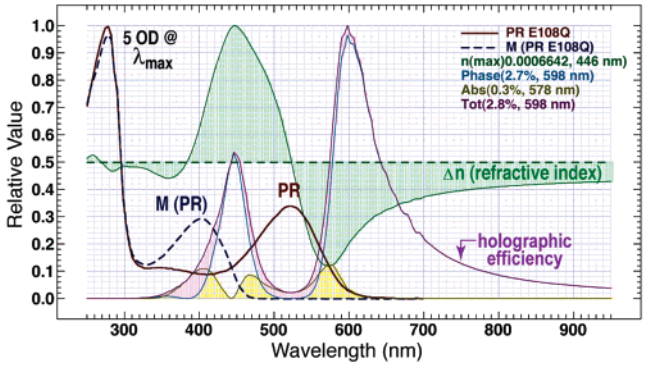

Figure 8. Wavelength dependence of the holographic diffraction efficiencies for (a) BR D96N and (b) GPR E108Q based on the Kramers−Kronig transform and the Kogelnik equations. The calculations are carried out assuming an optical density of 5 at the 280 nm protein peak and 50% photoconversion from the resting BR/PR state to M. Plotted as a function of wavelength, data for absorbance, the change in refractive index (Δn, the x-axis for this data has been shifted by +0.5 for clarity), and the diffraction efficiency, η, are normalized to their maximum values. The total diffraction efficiency is plotted along with its absorption and phase contributions; note that η is almost entirely dominated by the phase component. Although D96N is capable of higher diffraction efficiency, GPR E108Q requires lower writing intensities to achieve comparable diffraction efficiencies. The analysis is carried out by assuming that the resting state is pure bR (or PR) and the photochemically induced (blue) state is an equal mixture of the M state and the resting state (bR or PR).

shown) and is well described by a single exponential (although previous studies have indicated up to three components of the M state in this variant[41]). And just as observed for the wild-type protein, faster formation times result from higher writing intensities, while increased optical density slows formation of the diffraction pattern. Figure 8 illustrates the Kramers−Kronig and Kogelnik transforms for both GPR E108Q and BR D96N (see discussion below). Given the 647 nm reading wavelength, a diffraction efficiency of ∼1.3% should result for a film with an optical density of 5 at 280 nm ($OD_{520} \sim 1.7$). The measured value for an OD_{520} 2 film is 0.7% (Table 1), a difference of 46% from the predicted value.

In contrast to GPR E108Q, the equivalent variant for blue-absorbing proteorhodopsin shows poor holographic properties, characterized by a very low diffraction efficiency and a low signal-to-noise ratio (Figure 9). As expected, BPR E110Q exhibits a much slower response than the wild-type blue protein and a far greater sensitivity. The observed sensitivity is about an order of magnitude greater than the wild-type protein, as η_{max} is achieved with only about a tenth of the laser power required for BPR (Figure 6). However, the measured diffraction is about an order of magnitude lower, never exceeding ∼0.04% in a 1.4 OD_{490} film, and the resulting grating is not stable. The lifetime of the E110Q BPR photoactive state is the longest of

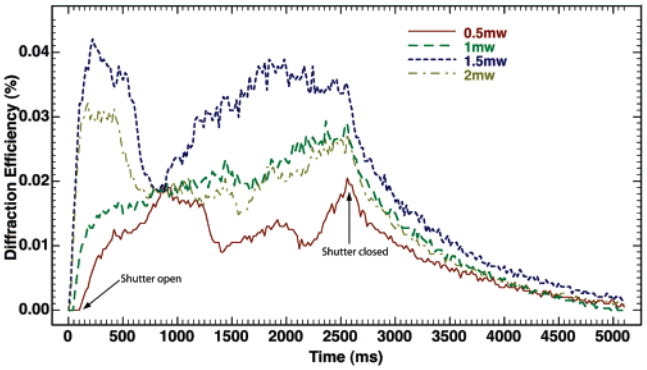

Figure 9. Blue proteorhodopsin E110Q diffraction data for a 1.4 OD film. The poor diffraction pattern probably results from the sample's extreme sensitivity to light, which results in unwanted photochemistry and therefore an unstable hologram.

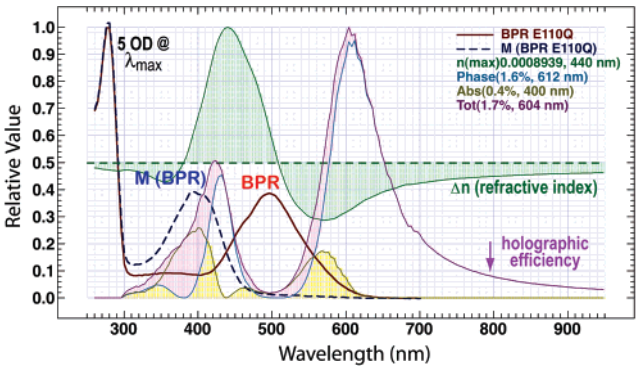

Figure 10. Wavelength dependence of the holographic diffraction efficiency for BPR E110Q based on the Kramers−Kronig transform and the Kogelnik equations. See explanation in the caption for Figure 8. The analysis is carried out by assuming that the resting state is pure BPR and the photochemically induced (blue) state is an equal mixture of the M state and the resting state (BPR). Just as for GPR E108Q, the diffraction efficiency is dominated by the contribution from the phase component.

all samples tested. Using the methods described earlier, it is estimated to be ca. 1800 ms, which is 3 times longer than observed for GPR E108Q (Table 1).

There are a number of plausible explanations for the poor diffraction reflected in the traces shown in Figure 9. A possible cause is the extreme sensitivity exhibited by the sample, which might degrade the integrity of interference fringes (i.e., reduce the grating contrast). Photoexcitation at 520 nm is 30 nm off-resonance from the BPR 490 nm λ_{max}, although this loss in efficiency is likely to be minimal.

The Kramers−Kronig and Kogelnik analyses for BPR E110Q shown in Figure 10 predict that the diffraction efficiency should be about 1.7% at 608 nm and close to 1% at 647 nm (for OD_{280} of 5, $OD_{490} \sim 1.9$). It is worth noting that the 647 nm reading wavelength is a better match for the BPR E110Q than for the equivalent GPR mutation, which is predicted to diffract best at 598 nm. Although the predicted diffraction efficiency is lower than that of GPR E108Q (Figure 8b vs Figure 10), the difference between theory and experiment is striking. While the comparison for GPR E108Q detailed above revealed a 46% difference, the gap between theory and experiment for BPR E110Q is much larger, approximately an order of magnitude smaller than might have been expected, even when the absorbance difference at 280 nm is considered (Table 1, 1.4 OD_{490} film, $\eta_{max} = 0.04\%$). The source of this discrepancy is not clear but most likely is the result of incomplete photoconversion; the Kramers−Kronig analysis assumes 50% of the protein in the M state. The lack

of contrast between fringes in the grating could result from poor photoconversion, light scattering, or problems with sample preparation. To confirm that the anomalous measurement originates from the sample and not the optical layout (e.g., problems with sample alignment, etc.), the wild-type GPR film was reexamined and yielded values consistent with those previously measured. In-house observations indicate that both the wild-type blue proteorhodopsin and the E110Q variant are particularly sensitive to sample preparation. Drift in pH and sample age can radically alter the protein's properties—preliminary results indicate that a drop in pH from 10 to 9 can inhibit M-state formation, especially in older samples (data not shown). The grating instability at all writing powers is a reflection of the poor signal-to-noise ratio—the variation evident in Figure 9 is of the same magnitude as the noise levels in Figures 4, 6, and 7 and might be due to simple light scattering in the poly(acrylamide) matrix. Once the shutter closes and blocks the writing beams, grating decay is well behaved, reflecting the fact that unlike grating formation, decay is not a dynamic process (Figure 9).

There are several factors that might explain the gap between the theoretically predicted and observed diffraction efficiencies for both proteins. Incomplete photoconversion will cause a deviation from ideal behavior, i.e., if insufficient M state is formed during grating formation. As mentioned above, the theoretical analysis in Figures 8 and 10 assumes a 50% photoconversion. While poly(acrylamide) is an excellent host for proteins, it is not a high-quality optical matrix and might scatter sufficient light to degrade the diffraction grating. Furthermore, the prolonged M states in these proteins may result in reduced grating contrast if stray or scattered light produces unwanted photoconversion to M across fringes.

Conclusions

Diffraction efficiency is a critical benchmark of the quality of a holographic material. With respect to holographic memory storage, a higher η translates into a better signal-to-noise ratio and a reduction of data loss. Diffraction efficiency is also related to the maximum data capacity of a given volume of multiplexed holographic media (dynamic range or M/#[58])—storage of multiple interference patterns through angular multiplexing inevitably reduces the η of previously stored data, so a higher η translates into greater storage density.

The discovery and ongoing characterization of the marine proteorhodopsins present the opportunity to evaluate these photoactive proteins for the same technologies targeted for bacteriorhodopsin. In this work the volume holographic diffraction efficiencies of four different proteorhodopsins are measured, including WT GPR and BPR, as well as their respective mutations E108Q and E110Q, and it is demonstrated for the first time that these proteins can be used as real-time holographic materials.

The wild-type green and blue proteorhodopsins form diffraction gratings readily with maximum observed efficiencies (η_{max}) of about 1% and 0.3%, respectively, for 1.7 OD films. In contrast to bacteriorhodopsin, however, diffraction from both GPR and BPR occurs from a late photocycle red-shifted intermediate analogous to the BR N or O state. This conclusion is based on the low relative yield of M in these proteins (compared to BR) at moderately high pH (9.5−10)[40,43,45] as well as in-house photokinetic characterizations. Although not attempted here, elevation of the pH over 12 substantially increases the yield of the PR M state at the expense of the N state;[43] as such, transient holography at that pH may well occur with diffraction originating entirely from M (studies in progress). Both proteins exhibited single-exponential decays of the diffraction grating indicating that only the red-shifted N-like state contributed to its formation. If the M state from either protein contributes to grating formation, the effect is too small to be observed. It should be noted that the 520 nm writing beam used in these experiments, while a sound choice for photoexcitation of both GPR and BPR may degrade diffraction efficiencies in these samples by driving the N-like state back to the respective green and blue pR resting states (GPR "N" $\lambda_{max} = 560$ nm[40] and BPR "N" $\lambda_{max} > 500$ nm from in-house observations and Wang et al.[45]). Dioumaev et al.[41] and Váró et al.[40] both report that formation of the N-like state is reversible, although it is not specified whether this state is photoactive. The safest approach to future experiments would be to select an actinic wavelength to the blue of the PR λ_{max}.

Of the four different PR samples, WT GPR produces the highest diffraction efficiency but also requires the highest writing intensity. GPR E108Q has the second highest diffraction efficiency and proved to be far more sensitive, requiring a writing intensity to reach η_{max} of only 1/100th of that needed for WT GPR. Because η_{max} generated from GPR E108Q is comparable to WT, but produced with far lower actinic intensities, this protein may prove to be competitive as a transient holographic medium. The blue absorbing wild-type and E110Q proteorhodopsins did not perform nearly as nicely as their green analogues, with the latter performing the most poorly in the group. WT BPR required about one-third to half of the actinic intensity required for GPR but produced a proportionally low η_{max} at a given optical density. And contrary to the GPR pair, where E108Q was found to be superior, BPR E110Q performed worse than the wild type with η_{max} nearly an order of magnitude lower (Table 1). On the basis of these results, it would seem that the BPR proteins are not suitable candidates for optical applications.

The question naturally arises as to whether proteorhodopsin, in general, is a better candidate for device applications than bacteriorhodopsin. Although it is too soon to answer this question unambiguously, a few points are worth noting. The differences in apparent stability and ease of production between these two proteins have been discussed above; all proteorhodopsins evaluated in the literature thus far (with the exception of that from *Pelagibacter* strain HTCC1062[5,59] and several flavobacteria[60]) have been produced heterologously in *E. coli* and as such can be produced much faster and in much higher yields than bacteriorhodopsin from *Halobacterium salinarum* (BR expressed heterologously behaves differently than wild type). And detergent-solubilized, trimeric[53] PR may result in higher quality optical materials that scatter light less than those containing purple membrane (although this has not proven to be a serious limitation for membrane-bound BR). With respect to whether GPR E108Q is superior to BR D96N, several factors bear consideration. E108Q will probably never match the maximum possible diffraction efficiency of D96N due to the smaller difference in λ_{max} between the PR resting and M states (~120 nm vs ~160 nm for BR). This assertion is supported by the Kramers−Kronig and Kogelnik analyses for the two proteins, shown in Figure 8. However, GPR E108Q requires approximately 1−2 orders of magnitude less power than D96N for writing a hologram (intensities of $10-10^2$ mW/cm^2 are typically reported for D96N[18,19,22,25,28]), which may make it a better candidate for some architectures. Furthermore, molecular biology techniques may be able to improve diffraction efficiency.

It is worth considering the applicability and commercial viability of dynamic holographic materials. Such materials have applications in real-time image and signal processing, telecommunications, switchable gratings, autocorrelators and associative memories,[18,20,28,56,57,61] and sensors.[62] The Fringemaker system marketed by Munich Innovative Biomaterials is a notable example (http://www.mib-biotech.de/[10]), which is capable of real-time nondestructive testing of manufactured components through microscopic deformation and interferometric analysis.

A bistable write−read−erasable system capable of permanent holographic operations is ultimately a desirable goal. Diffraction patterns written in materials based on BR D96N or PR E108Q last only as long as the lifetime of the M state in these proteins. In bacteriorhodopsin, the Q state, a 9-*cis*-retinal containing species produced in a branch off of the O state in the main photocycle, may fulfill that role,[14,36] and ongoing studies are being pursued to that effect. An equivalent state in proteorhodopsin has yet to be conclusively demonstrated. Mutations at PR D227 are promising; this residue (along with D97) plays a regulatory role in chromophore isomerization. Specifically, protonation of D227 at low pH facilitates formation of a long-lived blue-absorbing (430 nm) 9-cis species upon continuous illumination with green light, and mutation of this residue to asparagine enhances formation of the 430 nm state considerably (>50-fold).[63] Irradiation of PR D227N at high pH produces a long-lived 13-*cis* 362 nm state with a 30 min lifetime.[64] Either of these states may have potential for holographic architectures, with the advantage of longer-lived diffraction gratings, and may prove valuable in pointing the way toward variants with truly permanent bistable states. This goal might be achieved through site saturation or directed evolution studies—such efforts are currently being applied to bacteriorhodopsin with considerable success, having produced a several hundred-fold improvement in the efficiency with which the permanent state can be accessed.[32,38,39]

Finally, the potential of proteorhodopsin for device applications is just starting to be explored. Whereas the parent organism for BR, *Halobacterium salinarum*, has a fairly limited natural distribution, PR represents an incredibly diverse family of proteins that has proven to be ubiquitous in marine environments, produced by a wide variety of microbes;[2,3,5−7,46−50] the two recent expeditions by Venter and co-workers have identified thousands of gene sequences that code for proteorhodopsin variants. Whether this level of diversity is an advantage to device applications remains to be seen—the lack of naturally occurring BR variants has resulted in the highly focused mutagenesis studies referred to earlier, which is arguably a quicker route to success. However, the apparent diversity evident for PR may facilitate technologies not possible for BR. Such possibilities will become apparent as new PR variants are screened and characterized.

Acknowledgment. The authors gratefully acknowledge the support of the National Science Foundation (grants CCF-0432151 and CCF-0624695), Genencor International (a Danisco Company), and the Syracuse University W. M. Keck Center for Molecular Electronics.

Supporting Information Available: Details of the application of the Kramers−Kronig transformation and Kogelnik's coupled wave theory to the prediction of holographic properties for the photoactive proteins evaluated in this article. This material is available free of charge via the Internet at http://pubs.acs.org.

References and Notes

(1) Béjà, O.; Aravind, L.; Koonin, E. V.; Suzuki, M. T.; Hadd, A.; Nguyen, L. P.; Jovanovich, S. B.; Gates, C. M.; Feldman, R. A.; Spudich, J. L.; Spudich, E. N.; DeLong, E. F. *Science* **2000**, *289*, 1902.

(2) Man, D.; Wang, W.; Sabehi, G.; Aravind, L.; Post, A. F.; Massana, R.; Spudich, E. N.; Spudich, J. L.; Béjà, O. *EMBO J.* **2003**, *22*, 1725.

(3) Sabehi, G.; Massana, R.; Bielawski, J. P.; Rosenberg, M.; Delong, E. F.; Béjà, O. *Environ. Microbiol.* **2003**, *5*, 842.

(4) Béjà, O.; Spudich, E. N.; Spudich, J. L.; Leclerc, M.; DeLong, E. F. *Nature (London)* **2001**, *411*, 786.

(5) Giovannoni, S. J.; Bibbs, L.; Cho, J. C.; Stapels, M. D.; Desiderio, R.; Vergin, K. L.; Rappe, M. S.; Laney, S.; Wilhelm, L. J.; Tripp, H. J.; Mathur, E. J.; Barofsky, D. F. *Nature (London)* **2005**, *438*, 82.

(6) Venter, J. C.; Remington, K.; Heidelberg, J. F.; Halpern, A. L.; Rusch, D.; Eisen, J. A.; Wu, D.; Paulsen, I.; Nelson, K. E.; Nelson, W.; Fouts, D. E.; Levy, S.; Knap, A. H.; Lomas, M. W.; Nealson, K.; White, O.; Peterson, J.; Hoffman, J.; Parsons, R.; Baden-Tillson, H.; Pfannkoch, C.; Rogers, Y. H.; Smith, H. O. *Science* **2004**, *304*, 66.

(7) Rusch, D. B.; Halpern, A. L.; Sutton, G.; Heidelberg, K. B.; Williamson, S.; Yooseph, S.; Wu, D.; Eisen, J. A.; Hoffman, J. M.; Remington, K.; Beeson, K.; Tran, B.; Smith, H.; Baden-Tillson, H.; Stewart, C.; Thorpe, J.; Freeman, J.; Andrews-Pfannkoch, C.; Venter, J. E.; Li, K.; Kravitz, S.; Heidelberg, J. F.; Utterback, T.; Rogers, Y. H.; Falcon, L. I.; Souza, V.; Bonilla-Rosso, G.; Eguiarte, L. E.; Karl, D. M.; Sathyendranath, S.; Platt, T.; Bermingham, E.; Gallardo, V.; Tamayo-Castillo, G.; Ferrari, M. R.; Strausberg, R. L.; Nealson, K.; Friedman, R.; Frazier, M.; Venter, J. C. *PLoS Biol.* **2007**, *5*, e77.

(8) Burr, G. W. Holographic storage. In *Encyclopedia of Optical Engineering*; Johnson, R. B., Driggers, R. G., Eds.; Marcel Dekker: New York, 2003.

(9) Burr, G. W. *Proc. SPIE* **2003**, *5225-16.*

(10) Hampp, N.; Juchem, T. Fringemaker—the first technical system based on bacteriorhodopsin, Bioelectronic applications of photochromic pigments, Szeged, Hungary, 2000.

(11) Birge, B.; Fleitz, P.; Gross, R.; Izgi, J.; Lawrence, A.; Stuart, J.; Tallent, J. *Spatial light modulators and optical associative memories based on bacteriorhodopsin*; Materials Research Society: Boston, MA, 1990.

(12) Birge, R. R. *Annu. Rev. Phys. Chem.* **1990**, *41*, 683.

(13) Birge, R. R. *IEEE Comput.* **1992**, *25*, 56.

(14) Birge, R. R.; Gillespie, N. B.; Izaguirre, E. W.; Kusnetzow, A.; Lawrence, A. F.; Singh, D.; Song, Q. W.; Schmidt, E.; Stuart, J. A.; Seetharaman, S.; Wise, K. J. *J. Phys. Chem. B* **1999**, *103*, 10746.

(15) Stuart, J. A.; Marcy, D. L.; Wise, K. J.; Birge, R. R. Biomolecular electronic device applications of bacteriorhodopsin. In *Molecular Electronics: Bio-sensors and Bio-computers*; Barasanti, L. E. A., Ed.; Kluwer Academic Publishers: Dordrecht, 2003; p 265.

(16) Rayfield, G. Ultra high speed bacteriorhodopsin photodetectors. In *Molecular Electronics*; Hong, F. T., Ed.; Plenum: New York, 1989; p 361.

(17) *Molecular Electronics and Hybrid Computers*; Vought, B. W., Birge, R. R., Eds.; Wiley-Interscience: New York, 1999; Vol. 13, p 477.

(18) Hampp, N.; Bräuchle, C.; Oesterhelt, D. *Biophys. J.* **1990**, *58*, 83.

(19) Hampp, N.; Popp, A.; Bräuchle, C.; Oesterhelt, D. *J. Phys. Chem.* **1992**, *96*, 4679.

(20) Hampp, N.; Bräuchle, C.; Oesterhelt, D. *MRS Bull.* **1992**, *17*,, 56.

(21) Birge, R. R.; Izgi, K. C.; Stuart, J. A.; Tallent, J. R. *Proc. Mater. Res. Soc.* **1991**, *218*, 131.

(22) Zeisel, D.; Hampp, N. *J. Phys. Chem.* **1992**, *96*, 7788.

(23) Birge, R. R.; Fleitz, P. A.; Gross, R. B.; Izgi, J. C.; Lawrence, A. F.; Stuart, J. A.; Tallent, J. R. *Proc. IEEE EMBS* **1990**, *12*, 1788.

(24) Korchemskaya, E. Y.; Soskin, M. S.; Dyukova, T. V.; Vsevolodov, N. N. *SPIE* **1993**, *2083*, 217.

(25) Yao, B.; Ren, Z.; Menke, N.; Wang, Y.; Zheng, Y.; Lei, M.; Chen, G.; Hampp, N. *Appl. Opt.* **2005**, *44*, 7344.

(26) Bunkin, F. V.; Vsevolodov, N. N.; Druzhko, A. B.; Mitsner, B. I.; Prokhorov, A. M.; Savranskii, V. V.; Tkachenko, N. W.; Shevchenko, T. B. *Sov. Tech. Phys. Lett.* **1981**, *7*, 630.

(27) Gross, R. B.; Izgi, K. C.; Birge, R. R. *Proc. SPIE* **1992**, *1662*, 186.

(28) Thoma, R.; Hampp, N. *Opt. Lett.* **1992**, *17*, 1158.

(29) Downie, J. D.; Timucin, D. *Opt. Lett.* **1998**, *23*, 730.

(30) Oesterhelt, D.; Bräuchle, C.; Hampp, N. *Q. Rev. Biophys.* **1991**, *24*, 425.

(31) Yao, B.; Lei, M.; Ren, L.; Menke, N.; Wang, Y.; Fischer, T.; Hampp, N. *Opt. Lett.* **2005**, *30*, 3060.

(32) Hillebrecht, J. R.; Koscielecki, J. F.; Wise, K. J.; Marcy, D. L.; Tetley, W.; Rangarajan, R.; Sullivan, J.; Brideau, M.; Krebs, M. P.; Stuart, J. A.; Birge, R. R. *Nanobiotechnology* **2005**, *1*, 141.

(33) Fimia, A.; Acebal, P.; Murciano, S.; Blaya, S.; Carretero, L.; Ulibarrena, M.; Aleman, R.; Gomariz, M.; Meseguer, I. *Opt. Express* **2003**, *11*, 3438.

(34) Yoshida, M.; Ohno, K.; Takeuchi, Y.; Kagawa, Y. *Biochem. Biophys. Res. Commun.* **1977**, *75*, 1111.

(35) Vsevolodov, N. N.; Poltoratskii, V. A. *Sov. Phys. Tech. Phys.* **1985**, *30*, 1235.

(36) Popp, A.; Wolperdinger, M.; Hampp, N.; Bräuchle, C.; Oesterhelt, D. *Biophys. J.* **1993**, *65*, 1449.

(37) Gillespie, N. B.; Wise, K. J.; Ren, L.; Stuart, J. A.; Marcy, D. L.; Hillebrecht, J.; Li, Q.; Ramos, L.; Jordan, K.; Fyvie, S.; Birge, R. R. *J. Phys. Chem. B* **2002**, *106*, 13352.

(38) Wise, K. J.; Gillespie, N. B.; Stuart, J. A.; Krebs, M. P.; Birge, R. R. *Trends Biotechnol.* **2002**, *20*, 387.

(39) Hillebrecht, J. R.; Wise, K. J.; Koscielecki, J. F.; Birge, R. R. *Methods Enzymol.* **2004**, *388*, 333.

(40) Váró, G.; Brown, L. S.; Lakatos, M.; Lanyi, J. K. *Biophys. J.* **2003**, *84*, 1202.

(41) Dioumaev, A. K.; Brown, L. S.; Shih, J.; Spudich, E. N.; Spudich, J. L.; Lanyi, J. K. *Biochemistry* **2002**, *41*, 5348.

(42) Friedrich, T.; Geibel, S.; Kalmbach, R.; Chizhov, I.; Ataka, K.; Heberle, J.; Engelhard, M.; Bamberg, E. *J. Mol. Biol.* **2002**, *321*, 821.

(43) Szakács, J.; Lakatos, M.; Ganea, C.; Váró, G. *J. Photochem. Photobiol. B* **2005**, *79*, 145.

(44) Dioumaev, A. K.; Wang, J. M.; Balint, Z.; Varo, G.; Lanyi, J. K. *Biochemistry* **2003**, *42*, 6582.

(45) Wang, W. W.; Sineshchekov, O. A.; Spudich, E. N.; Spudich, J. L. *J. Biol. Chem.* **2003**, *278*, 33985.

(46) de la Torre, J. R.; Christianson, L. M.; Béjà, O.; Suzuki, M. T.; Karl, D. M.; Heidelberg, J.; DeLong, E. F. *Proc. Natl. Acad. Sci. U.S.A.* **2003**, *100*, 12830.

(47) Kelemen, B. R.; Du, M.; Jensen, R. B. *Biochim. Biophys. Acta* **2003**, *1618*, 25.

(48) Man-Aharonovich, D.; Sabehi, G.; Sineshchekov, O. A.; Spudich, E. N.; Spudich, J. L.; Béjà, O. *Photochem. Photobiol. Sci.* **2004**, *3*, 459.

(49) Bielawski, J. P.; Dunn, K. A.; Sabehi, G.; Béjà, O. *Proc. Natl. Acad. Sci. U.S.A.* **2004**, *101*, 14824.

(50) Sabehi, G.; Béjà, O.; Suzuki, M. T.; Preston, C. M.; DeLong, E. F. *Environ. Microbiol.* **2004**, *6*, 903.

(51) Hillebrecht, J. R.; Galan, J.; Rangarajan, R.; Ramos, L.; McCleary, K.; Ward, D. E.; Stuart, J. A.; Birge, R. R. *Biochemistry* **2006**, *45*, 1579.

(52) Dencher, N. A.; Heyn, M. P. *Methods Enzymol.* **1982**, *88*, 5.

(53) Liang, H.; Whited, G.; Nguyen, C.; Stucky, G. D. *Proc. Natl. Acad. Sci. U.S.A.* **2007**, *104*, 8212.

(54) Reynolds, J. A.; Stoechenius, W. *Proc. Natl. Acad. Sci. U.S.A.* **1977**, *74*, 2803.

(55) Bräuchle, C.; Burland, D. M. *Angew. Chem., Int. Ed. Engl.* **1983**, *22*, 582.

(56) Wolperdinger, M.; Hampp, N. *Biophys. Chem* **1995**, *56*, 189.

(57) Hampp, N.; Bräuchle, C.; Oesterhelt, D. Mutated bacteriorhodopsins: new materials for optical storage and information processing. 4th International Symposium on Bioelectronic and Molecular Electronic Devices, Miyazaki, Japan, 1992.

(58) Burr, G. W.; Psaltis, D. *Opt. Lett.* **1996**, *21*, 896.

(59) Stingl, U.; Desiderio, R. A.; Cho, J. C.; Vergin, K. L.; Giovannoni, S. J. *Appl. Environ. Microbiol.* **2007**, *73*, 2290.

(60) Gomez-Consarnau, L.; Gonzalez, J. M.; Coll-Llado, M.; Gourdon, P.; Pascher, T.; Neutze, R.; Pedros-Alio, C.; Pinhassi, J. *Nature (London)* **2007**, *445*, 210.

(61) Renner, T.; Hampp, N. *Opt. Commun.* **1993**, *96*, 142.

(62) Ye, H.; Nilsen, O.; Bright, V. M.; Anderson, D. Z. *Opt. Lett.* **2005**, *30*, 1467.

(63) Imasheva, E. S.; Balashov, S. P.; Wang, J. M.; Dioumaev, A. K.; Lanyi, J. K. *Biochemistry* **2004**, *43*, 1648.

(64) Imasheva, E. S.; Shimono, K.; Balashov, S. P.; Wang, J. M.; Zadok, U.; Sheves, M.; Kamo, N.; Lanyi, J. K. *Biochemistry* **2005**, *44*, 10828.